Biomedicine & Pharmacotherapy 158 (2023) 114141

Contents lists available at ScienceDirect

Biomedicine & Pharmacotherapy

journal homepage: www.elsevier.com/locate/biopha

Identification of a novel adiponectin receptor and opioid receptor dual acting agonist as a potential treatment for diabetic neuropathy

Oscar Ka-Fai Ma [a,1], Simone Ronsisvalle [b,1], Livia Basile [b], Ariya Weiman Xiang [a], Cristina Tomasella [b], Federica Sipala [b], Matteo Pappalardo [b], Koon-Ho Chan [a], Danilo Milardi [c], Roy Chun-Laam Ng [a,*], Salvatore Guccione [b,*]

[a] Department of Medicine, LKS Faculty of Medicine, The University of Hong Kong, Hong Kong Special Administrative Region
[b] Department of Drug and Health Science, University of Catania, Viale A.Doria 6 ed.2, I-95125 Catania, Italy
[c] CNR (National Research Council of Italy) – Institute of Crystallography, Via Paolo Gaifami 18, I-95126 Catania, Italy

ARTICLE INFO

Keywords:
Adiponectin
AdipoR agonist
Benzomorphanic derivatives
Opioid receptors
Diabetic Neuropathy

ABSTRACT

Diabetic neuropathy (DN) is a long-term complication of diabetes mellitus, affecting different periphery nerve systems including sensory and motor neurons. Hyperglycemia is the major cause of DN with symptoms such as weakness of balance or coordination, insensitivity to sensation, weakness of the muscles as well as numbness and pain in limbs Analgesic drug such as opioids can be effective to relief neuropathy pain but there is no effective treatment. Adiponectin is an anti-diabetic adipokine, which possesses insulin-sensitizing and neuroprotective effects. In this project, we aim to identify an agent which is dual acting to opioid and adiponectin receptors. Within a virtual screening repositioning campaign, a large collection of compounds with different structures comprehensive of adipoRon-*like* piperidine derivatives was screened by docking. Recently developed opioid receptor benzomorphanic agonists finally emerged as good ligands to adiponectin receptors showing some 2D and 3D structural similarities with AdipoRon. Particularly, we have identified (+)-MML1017, which has high affinity to the same binding domain of AdipoR1 and AdipoR2 as AdipoRon. Our western blot results indicate (+)-MML1017 activates AMPK phosphorylation through both adipoR1 and adipoR2 in neuronal cell line. Moreover, pretreatment of (+)-MML1017 can improve the cell viability with motor neurons under hyperglycermic conditions. The (+)-MML1017 also activates μ-opioid receptor cells in a concentration-dependent manner. Our study identified a novel compound having dual activity on opioid receptors and adiponectin receptors that may have analgesic effects and neuroprotective effects to treat diabetic neuropathy.

1. Introduction

Diabetic neuropathy (DN) is one of the most common complications of diabetes mellitus that affects more than 50% of diabetic patients including both type 1 diabetes mellitus (T1DM) and type 2 diabetes mellitus (T2DM) [1]. Diabetic patients may suffer from extensive nerve damage and dysfunction in periphery without any overt symptoms. DN primarily affects sensory nerves in which patients commonly experience sensory symptoms including pain, prickling and tingling sensation. It also affects motor neurons leading to weakness of the toes and ankles [2]. The progressive impairment results in loss of lower extremity sensation and motor weakness. The molecular mechanisms underlying DN and the onset and progression of nerve damage is not fully understood. Moreover, it is unfortunate that there is no curative treatment for diabetic neuropathy other than glycemic control.

Neuropathic pain is a common symptom of DN in which the peripheral sensory neurons are impaired with multifactorial etiology including oxidative stress, inflammation, and finally neuronal apoptosis [3–5]. Opioid analgesics have in fact less efficacy in diabetic neuropathy treatment and tolerance rapidly occurs after chronic usage [6].

Abbreviations: ADIPOR1/2, Adiponectin Receptor 1/2; APN, Adiponectin; AMPK, AMP-activated Protein Kinase; DN, Diabetic neuropathy; DOR, δ-opioid receptor; IL1β, Interleukin 1β; KOR, κ-opioid receptor; MOR, μ-opioid receptor; MTT, 3-(4, 5-dimethylthiazolyl-2)-2, 5-diphenyltetrazolium bromide; T2DM, Type 2 Diabetes Mellitus; TNFα, Tumor Necrosis Factorα.

* Corresponding authors.
E-mail addresses: royclng@hku.hk (R.C.-L. Ng), salvatore.guccione@unict.it (S. Guccione).
[1] Co-first author

https://doi.org/10.1016/j.biopha.2022.114141
Received 3 October 2022; Received in revised form 3 December 2022; Accepted 13 December 2022

Neuropathies provoke, in a large number of cases, excessive sensitivity to nociceptive stimuli or make perceptible as painful normal stimuli. Nevertheless, opioid analgesics have been used to treat diabetic pain. Opioid analgesia is modulated through three GPCRs, named μ-opioid receptor (MOR), δ-opioid receptor (DOR), and κ-opioid receptor (KOR). It was reported that opioids combining MOR agonist–DOR antagonist activity may be a more effective antinociceptive agent in which MOR-mediated side effects are attenuated [7]. The reduction of opioid analgesics efficacy and side effects in this type of pain might be due to MOR in the spinal cord. Recently, searching for alternate μ-opioid receptors antinociceptive pathways different from that one's well-known signal transduction mediated, some of us described benzomorphan derivatives that are μ-opioid receptor ligands and do not possess any affinity for the other opioid receptor subclasses delta and kappa [8–10]. However, an agent which only possesses an analgesic effect can ameliorate pain symptoms in DN but may not be able to treat DN. Multi-target drugs have emerged to treat diabetic neuropathy due to the complex etiology and its multifactorial pathogenesis.

Adiponectin (APN) is a circulatory adipokine predominantly secreted from adipocytes and the liver, possessing insulin-sensitizing, anti-inflammatory, and anti-oxidative effects [11,12]. It has been associated with type 2 diabetes mellitus (T2DM) and diabetes complications [11]. APN binds to adiponectin receptors (ADIPOR1 and ADIPOR2) to sensitize insulin signaling and modulate fat metabolism. Low circulatory APN level can result in insulin resistance and accelerates the progression of diabetic symptoms. Studies indicate that genetic polymorphisms of adiponectin associated with lower circulatory APN levels increase the susceptibility to diabetic neuropathy [13,14]. Increasing evidence indicates that APN possesses neuroprotective effects in both central and peripheral nervous systems [15–18]. APN protects against neuronal death in retinal ganglion cells, hippocampal neurons, and sensory neurons in the hypothalamus [16,19,20]. A clinical study has also demonstrated that APN is associated with subclinical inflammation and sensorimotor nerve conduction in T1DM and T2DM patients [21]. More importantly, APN regulates thermal nociception in a mouse model of neuropathic pain. Adiponectin receptors are expressed in the neurons of somatosensory cortex, spinal cord dorsal horn, and glial cells in the spinal cord [18]. Loss of APN in mice resulted in exacerbated thermal insensitivity, which is associated with the elevation of proinflammatory cytokines (TNFα and IL1β) levels in the dorsal horn of the spinal cord [18]. These indicate that APN may regulate nociception by inhibiting neuroinflammation in the somatosensory nervous system [18]. Apart from the damages of sensory nervous system, neuronal loss and degeneration have been observed in motor system of both diabetic rodent models and diabetic patients [22,23], probably through oxidative stress in the motor neurons [24,25]. Adiponectin has been demonstrated with anti-oxidative and neuroprotective effects [15,16]. Activation of adiponectin signaling may protect neuronal loss in the sensorimotor system. AdipoRon has been identified as an orally active adiponectin receptor agonist demonstrating anti-diabetic effects and prolonged

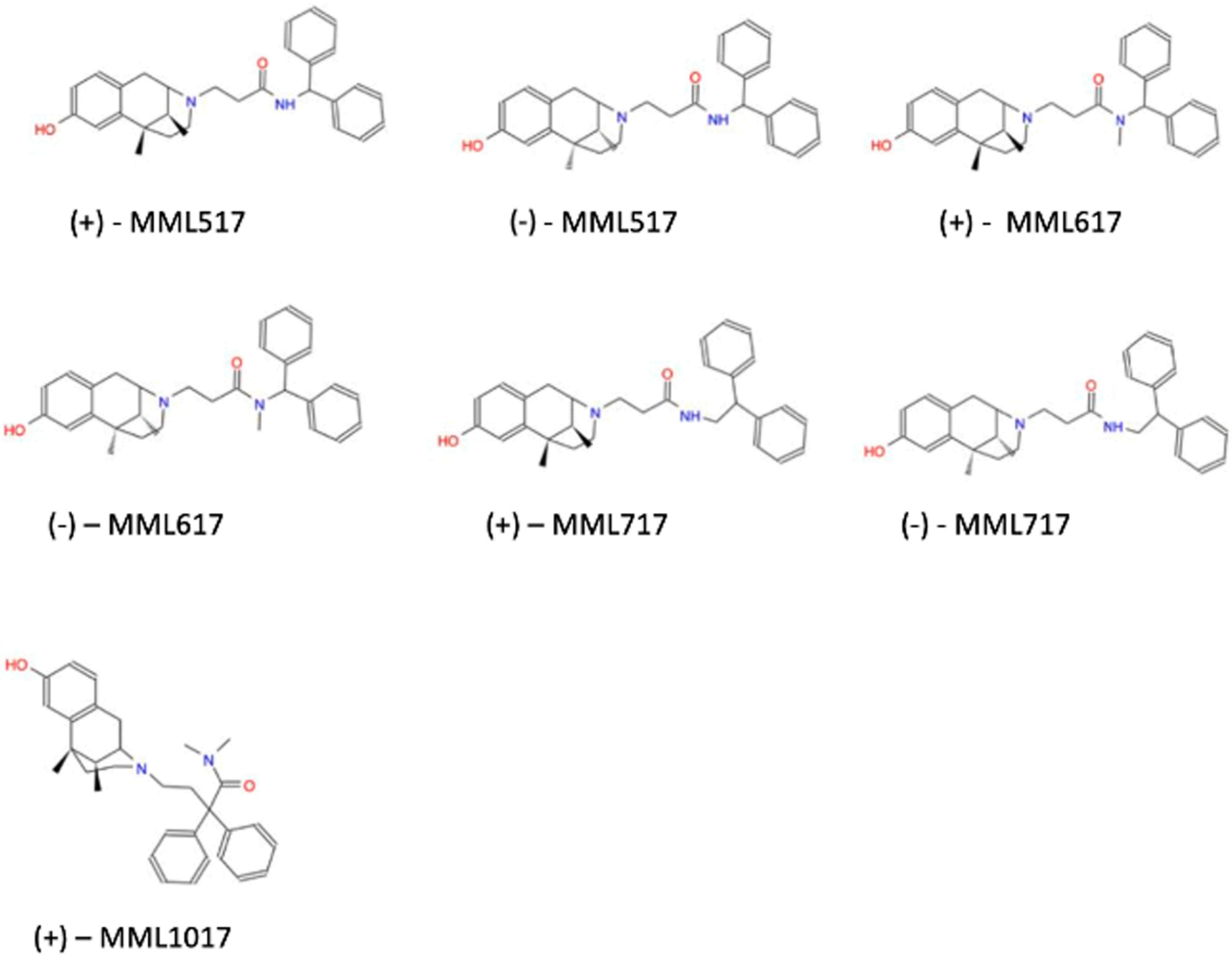

Fig. 1. Benzomorphan derivatives. The chemical structure of the benzomorphan derivatives that possess opioid binding affinity and being tested for ADIPO-R1, and -R2 binding.

shortened lifespan in obese diabetic mice [26]. It has also been applied to protect mouse models from neurodegeneration [27,28]. However, similar to some AMPK activators, it may inhibit mitochondrial functions and reduce ATP production which may worsen neuropathic pain [29]. Therefore, the identification of a novel adiponectin receptor agonist is essential for the adiponectin-based strategy to treat diabetic neuropathy.

Further to a virtual screening repositioning campaign comprehensive of previously reported benzomorphan derivatives and adipoRon-*like* piperidine derivatives by docking into ADIPO-R1 and -R2, benzomorphan derivatives endowed with opioid activity emerged as potential binders to ADIPO-R1 and -R2 (Fig. 1). Based on the docking score, the structural similarities with AdipoRon (unpublished results), and the good functional in vivo pharmacological profile, compound (+)-MML1017 [7] was finally chosen to be further tested as ADIPO-R ligand. Compound (+)-MML1017 might represent an exemplary dual-acting highly specific compound that can modulate the activity of the MOR system to manage neuropathic pain and able to activate adiponectin receptors for neuroprotection. *In vitro* study indicates that (+)-MML1017 induces AMPK phosphorylation through both ADIPO-R1 and ADIPO-R2 in motor neuron NSC-34 and increases the cell viability of neurons under hyperglycemic condition.

2. Materials and methods

2.1. Synthesis of Benzomorphan derivatives

Compounds were synthesized as previously reported [8–10]. Each compound was diluted in dimethyl sulfoxide (DMSO) to 100 mM and stored as stock at − 20 °C. Different concentrations were obtained by diluting the stock solution in phosphate-buffer saline (PBS) for cell culture. For the synthesis of + (-)MML-1017, in brief, The *N*-substituted *cis*-(+)-*N*-normetazocine derivative (+)-MML717 was obtained by alkylation of *cis*-(+)-*N*-normetazocine in anhydrous MeOH with the bromoamide 3-Bromo-N-(diphenylmethyl)propanamide. The alkylation procedure was performed in the dark under argon atmosphere in anhydrous MeOH at 50 °C using $NaHCO_3$ and KI. After cooling at room temperature, the solvent was removed in vacuo and then extracted with dichloromethane [5]. Compound (+)-MML1017 was synthesized by heating under reflux for 16 h under an argon atmosphere in the dark a mixture of *cis*-(+)-*N*-normetazocine, dimethyl-(tetrahydro-3,3-diphenyl-2-furylidene)-ammonium bromide, anhydrous K_2CO_3 in CH_3CN. After cooling at room temperature, the solvent was removed in vacuo. Subsequently, the residue was extracted with dichloromethane. Evaporation under reduced pressure gave the crude compound, which was purified by flash chromatography on silica gel (CH_2Cl_2 and methanol as eluent). The collected fractions were combined, and the solvent was removed in vacuo to give the compound as a colorless crystalline solid [7].

2.2. Molecular docking and screening of adiponectin receptor agonist candidates

Marvin was used for drawing, displaying and characterizing chemical structures, substructures and reactions, Marvin version 21.17, 2019 ChemAxon (http://www.chemaxon.com). Docking studies were carried out on a Macintosh HD PC equipped with an 2,4 GHz Intel Core i5 quad-core. Gold Software (V. 2020.3) [30] was used to perform the docking of the benzomorphan derivatives into the X-ray structure of the adiponectin receptors (PDB code: 6KS0 and 6KS1; resolution 2.73 and 2.4 respectively). GOLD (V.2020.3) is a search approach based on a genetic algorithm with a workflow of four related steps. (i) Random setting up of a population of potential binding poses at the defined binding pocket. (ii) Encoding each member of a population as a "chromosome", which brings information about the protein–ligand interactions feature. (iii) A fitness score is assigned based on the chromosome predicted binding affinity, which is also a ranking criterion within the population. (iv) The population of chromosomes is iteratively optimized. In this study, the following genetic algorithm parameters were used: population size, 100; selection pressure, 1.1; number of islands, 5; migrate, 10; mutate, 95; crossover, 95; niche size, 5; and number of operations, 100000. Default cutoff values of 2.5 Å (dH–X) for hydrogen bonds and 4.0 Å for the van der Waals distance were employed. Allow early termination was set off. Generate diverse solution option was set at cluster size 1, R.M.S.D 1 Å. High quality 3D images of the complexes were visualized by Discovery Studio to identify the main interactions in the ligand-receptor complexes which were converted to 2D diagrams by the same software [31].

The search efficiency was set to its maximal value to increase the reliability of the docking results. In the GOLD docking algorithm, active site residues for both receptor states were selected as derived from MD trajectories. The defined residues were treated as flexible, and their side chains were rotated in 10° increments and scanned over 360°. Two docking scoring functions were used namely CHEMPLP fitness (for docking) which is an empirical fitness functions optimized for pose prediction and ChemScore (for rescoring) fitness function which takes account of hydrophobic-hydrophobic contact area, hydrogen bonding and ligand flexibility by incorporating ΔG, protein-ligand atom clash term, and an internal energy term. The scoring functions were used both with default parameters.

According to ligand interaction maps of the representative complexes [32] the analysis was focused on the interaction with key amino acids such as ARG267 - PHE271 - TYR310 for the interactions at ADIPOR1 and ARG278 - PHE282 - TYR321 for the interactions at ADIPOR2 (Supplementary Table1).

Since no open-form 3D structure of ADIPO-R2 is available in the Protein Data Bank (PDB) (https://www.rcsb.org/) for docking purposes an open structure was generated by Molecular Dynamics (MD). ADIPO-R1 was used as reference model to set the time required for the structure to switch from the closed to the open conformation. Comparative analysis of the open structure of ADIPO-R1 after MD with that available in PDB (PDB entry = 6KS0) allowed us to evaluate the time required to obtain the open conformation of adiponectin R2 starting from the closed form.

Human ADIPO-R1 D208A mutant (PDB entry = 6KRZ) and human ADIPO-R2 crystal structures (PDB entry = 6KS1) were used for Molecular Dynamics simulations. The amino acid Ala208 of the human adiponectin receptor 1 D208A mutant (PDB entry = 6KRZ) was mutated to Asp208 by PyMOL Molecular Graphics System (v0.9 Schrödinger, LLC) (http://www.pymol.org), and minimized using the conjugate gradient algorithm [33–35] before MD simulations.

Visual Molecular Dynamics (VMD) v. 1.9.3 was employed to prepare the input files and analyse the trajectories [36]. MD calculations were carried out using NAMD2 software (version 2.9) [37] with CHARMM22 (Chemistry at Harvard Macromolecular Mechanics) as forcefield [38]. The ion concentration was set to 0.3 M. Values of 12 and 14 Å were selected to calculate the Born radii and non-bounded forces, respectively. For the water solvent the GBIS (Generalized Born implicit solvent) model as implemented in NAMD was adopted [39,40]. The simulations were performed in ensemble number of particles- temperature kept constant at 310∘K. Systems were coupled with a Langevin thermostat to keep temperature under control. The SHAKE algorithm with a tolerance of $1 \times 10 - 8$ Å was used to fix the length of the covalent hydrogen bonds [66]. The non-bonded short-range interactions cut-off was set to 14 Å.

2.3. Cell culture

NSC-34 mouse motor neuronal cells were cultured in Dulbecco's modified Eagle's medium (DMEM) (Gibco) with 10% fetal bovine serum (FBS) (Invitrogen, USA) and 1% penicillin/streptomycin (Gibco). The cells were grown in a humidified incubator at 37 °C with 5% CO_2. Drug candidates were dissolved in DMSO and used for cell treatment. Concentration-dependent assay was performed to obtain the optimal

concentration for activating AMPK. To knockdown adiponectin receptors expression, mouse AdipoR1 and AdipoR2 siRNAs and non-targeting control siRNA were purchased from Santa Cruz Biotechnology. NSC-34 cells were seeded in a six-well tissue culture plate until 80% confluency. Then, NSC-34 cells were transfected with siRNA using lipofectamine 3000 reagent (Invitrogen, USA). The mixture of siRNA duplex and reagent was diluted in Opti-MEM medium (Gibco) and incubated at RT for 45 min. Then, the siRNA duplex and reagent mixture were added to NSC-34 cell. After 6-h incubation, medium containing siRNA was removed, and cells were further cultured for 18 h for western blot analysis.

2.4. Cell viability assay for neuronal survival in hyperglycemia condition

Neuronal cells were seeded onto 96-well plate with density of 5×10^4. The cells were starved for 3hrs and pretreated with (+)-MML1017 [8–10] for 3 h prior to incubation of glucose (Control: 5.5 mM and hyperglycermia condition: 30 mM). After 48 h incubation, the cell viability was assessed with 3-(4,5-dimethylthiazol-2-yl)2, 5-diphenyl-tetrazolium bromide (MTT) assay for the high glucose culture condition. Subsequently, each culture well was added with 20 μL MTT (0.5 mg/mL) and placed at 37 °C for 4 h. Then, the medium was removed carefully and 150 μL DMSO was added in each well. The absorbance was determined at a wavelength of 570 nm using a microplate reader a CLARIO star microplate reader (BMG LABTECH, Germany) as described by the manufacturer. Cell viability was expressed as a percentage of viable cells obtained relative to that of controls.

2.5. Protein extraction for western blotting

NSC-34 cells were washed with ice-cold phosphate-buffered saline (PBS) and lysed with 100 µl ice-cold lysis buffer (Cell Signaling Technology, USA) for 20 min with gentle shaking. Then, the lysates were centrifuged at 14,000g for 10 min at 4 °C, followed by collecting supernatant within cytosolic protein fraction. The protein concentration was quantified using the Bradford assay (BioRad, USA).

2.6. Calcium influx assay

hMOR-chem5 cells (Millipore, USA) were maintained as described by manufacturer protocol. In brief, cells were plated at 40,000 cells per well into a clear bottom black wall 96-well plate for overnight. The growth media was then decanted. Fluo-8 calcium flux assay kit (abcam, UK)) was performed to study the calcium flux. Cells were incubated with 100 mL of dye-loading solution for 1 h at room temperature. The cells were then incubated with or with 10 mM Bevenopran (MedChemExpress, USA) for 30 mins. Plates were read on a CLARIOstar Plus microplate reader (BMG Labtech, Germany) at 490/525 ex/em for a total of 5 mins. After30 s of readings, the cells were then incubated with different concentration of (+)-MML1017 in triplicate. Changes in Ca^{2+} flux were monitored, and peak height values were recorded. ΔRFU of different treatment groups were calculated by subtracting the maximum and minimum reading. The ΔRFU were subjected to nonlinear regression to determine the concentration response.

2.7. Western blot analysis

Cell homogenates (20 µg/well) were loaded onto 10% SDS polyacrylamide gels in denaturing conditions at 80 mA for 90 min and transferred electrophoretically (100 mA/blot, 2 h; Power Pack; Bio-Rad Laboratories, Inc., USA) to polyvinylidene fluoride (PVDF) membrane. Immunoblotting was performed as conventional method. Nonspecific binding was blocked with 5% non-fat milk powder in Tris-buffered saline-Tween containing 0.1% Tween-20 (PBS-T) for 1 h. Primary antibodies including rabbit anti-AdipoR1 (1:1000, Abcam, Cambridge, MA, USA), rabbit anti-AdipoR2 (1:1000, Boster Biological Technology, USA), rabbit anti-AMPK (1:1000, Cell Signaling Tech. Inc., USA), rabbit anti-p-$AMPK^{T172}$ (1:1000, Cell Signaling Tech. Inc., USA) antibody were incubated at 4 °C overnight, followed by HRP-conjugated secondary antibodies (goat anti-rabbit, 1:5000 or rabbit anti-mouse, 1:5000; Dako, Glostrup, Denmark) at RT for 1 h. The immunoblot signals were visualized by Westernbright Quantum HRP substrate (advansta, USA). Adiponectin receptors expression was examined to check the efficiency of siRNA transfection.

2.8. Statistical analysis

Densitometric analysis of the western blot results was performed by Image J software. Statistical analyses were performed by Prism 6 (GraphPad Software, Inc., La Jolla, CA, USA). Quantitative data were expressed as mean ± standard errors of the mean (S.E.M.) and analyzed using one-way ANOVA followed by post hoc comparison using Tukey's test. The difference was statistically significant when $p < 0.05$.

3. Results

3.1. Docking

AdipoRon (Fig. 2A) is the first non-peptide ligand discovered to interact at ADIPO-R1 and ADIPO-R2 with a higher affinity for ADIPO-R1. Therefore, the AdipoRon docking was performed as a reference. AdipoRon interacts with ADIPO-R1 and gives rise to an unconventional hydrophobic bond (Alkyl) with ILE212, a π -Hydrophobic Bond with TYR209 and TYR310, a mixed Hydrophobic Bond (Alkyl and π − Hydrophobic Bond) with ILE216, PHE 271, and a Hydrogen Bond with ARG 267 (Fig. 2B). Several interactions are formed at ADIPO-R2 with TYR220 (π- Hydrophobic Bond), ILE223, ARG 278, LEU320 and TYR 328 (mixed Hydrophobic Bond-Alkyl and π-Hydrophobic Bond), GLY324 (Hydrogen Bond). GOLD scorings were 90.63 and 77.19 at ADIPO-R1 and ADIPO-R2, respectively. Our result is in agreement with a previous study showing that AdipoRon preferentially binds to ADIPO-R1 with respect to ADIPO-R2 [41].

Based on the GOLD higher and quite comparable docking scores (Supplementary Table 1) therefore the potential ADIPO -R1 and -R2 affinity for two compounds namely (+)-MML1017 (score: 88.72) and (+) - MML717 (score:89.73) [8] emerged for a further pharmacological investigation (Supplementary Table 1) but finally the former compound was selected by virtue of its better activity i.e. functional in vivo profile at µ receptor system (*unpublished results*). The activity of compound (+) - MML717 [8] was really very poor in in vivo functional assays at the µ receptor system (*unpublished results*). The relevant (+)+ enantiomer of (+)-MML1017 [10] is not reported to be part of the ongoing patent).

(+)-MML1017 (score 88.72) binds in the same pocket at ADIPO-R1 as AdipoRon (Fig. 3A, F). interacting with the key residues (ARG267, PHE271, TYR310) (Fig. 3E,F) [32]. A π-π hydrophobic bond and a hydrophobic bond are formed by both AdipoRon and (+)-MML1017 with TYR310 and with ARG367, respectively (Fig. 3D, E, F). A quite similar situation (Fig. 4A) can be depicted i.e. same binding pocket at the ADIPOR-2 although (+)-MML1017 is better scored than AdipoRon. (80.95 vs. 77.19) (Fig. 4A) probably due to its capability to interact with the key residues (PHE282, TYR321) [32] (Fig. 4E and F), whereas AdipoRon does not interact with the aforementioned residues (Fig. 4D, F). A mixed π-alkyl hydrophobic and a π-hydrophobic interaction are established with TYR321 and PHE 282 respectively. Additional hydrophobic interactions are established with other amino acids in the active site of ADIPO-R2 namely ILE233, LEU226, TYR328, LEU 320, ALA 325, and VAL 335. In contrast, only a mixed π-alkyl hydrophobic interaction takes place with a key residue (ARG278) by AdipoRon [32]. These results indicate that (+)-MML1017 binds to the same domain of ADIPOR1 and ADIPOR2 as AdipoRon but it is a stronger binder than AdipoRon.

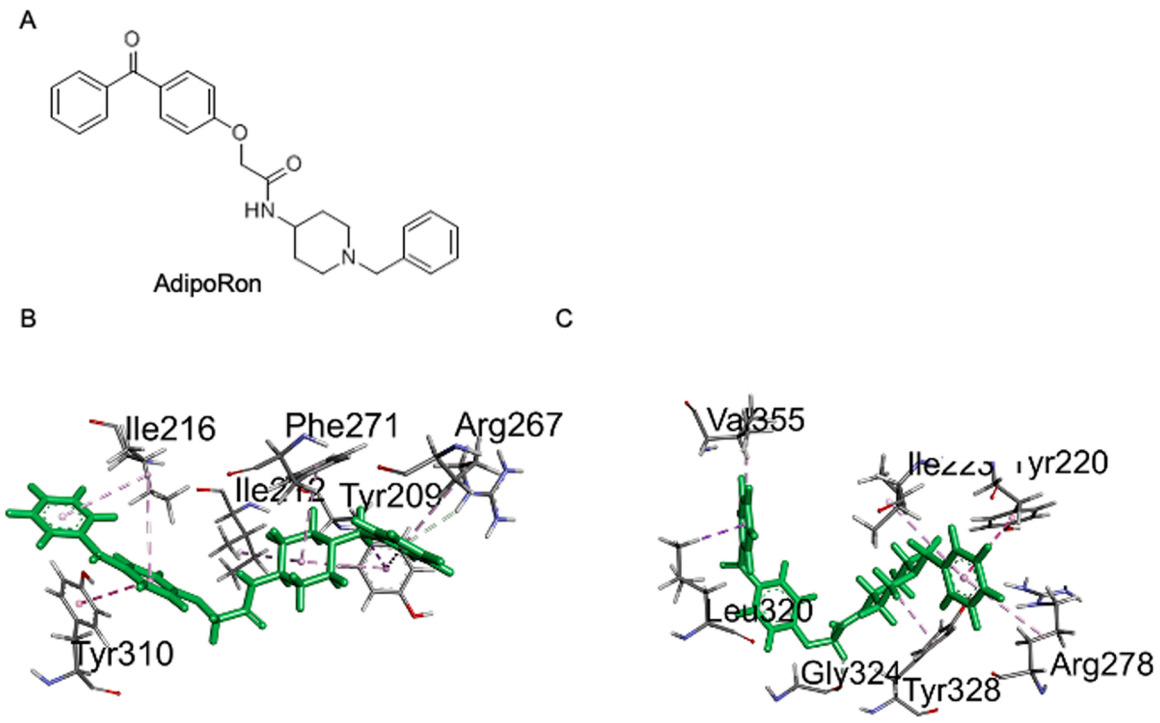

Fig. 2. Interaction between AdipoRon and adiponectin receptors. A. Chemical structure of AdipoRon. B. Interaction between ADIPOR-1 and the best pose of AdipoRon. AdipoRon is shown as green sticks with explicit hydrogen atoms and amino acid residues as gray lines. C. Interaction of AdipoRon (best pose) and ADIPO-R2. AdipoRon is shown as green sticks with explicit hydrogen atoms and amino acid residues as gray lines.

3.2. (+)-MML1017 induces ADIPORs-mediated AMPK activation

AMPK is the downstream cytoplasmic mediator of adiponectin signaling [42,43]. Upon activation, AMPK is phosphorylated at Thr172 that further activates cellular processes including insulin sensitization, autophagic degradation, fatty acid oxidation, cell proliferation and differentiation [44]. To examine if (+)-MML1017 can induce AMPK activation, NSC-34 neuronal cells were cultured with different concentration of (+)-MML1017 (0, 10, 25 nM) for 30 min. Protein lysates were isolated for western blot analysis. We found that $pAMPK^{Thr172}$ levels were increased in the presence of (+)-MML1017 (Fig. 5A). The increase of AMPK phosphorylation was in a concentration-dependent manner and most significantly induced at a ligand concentration of 25 nM (Fig. 5B). Thus, 25 nM was chosen as the concentration for the latter experiments. To further confirm if (+)-MML1017 activated AMPK through adiponectin receptors, we used siRNA to knock down AdipoR1 or AdipoR2 in NSC-34 cells prior to (+)-MML1017 treatment. The ability of (+)-MML1017 to induce AMPK phosphorylation was abolished in both ADIPOR1 siRNA-transfected and ADIPOR2 siRNA-transfected neuronal cells (Fig. 5C and E). The reduction of pAMPK/AMPK ratio in siAdipoR1 cells was about 22.5% while that of siAdipoR2-treated cells was about 82% (Fig. 5D and F). These indicated that (+)-MML1017 activates AMPK predominantly through AdipoR2. These data indicated that (+)-MML1017 induces AMPK phosphorylation in neurons through ADIPOR1 and ADIPOR2.

3.3. (+)-MML1017 enhances neuronal survival in hyperglycemic condition

High glucose level is the cause of neuronal apoptosis leading to diabetic neuropathy. Moreover, activation of AMPK can abate hyperglycemia-induced neuronal injury in the DN mouse model [45]. In recent report, high glucose condition reduces cell viability of NSC-34 motor-like neuron that is associated with diabetic neuropathy [46]. Hyperglycemia generates advanced glycation end products (e.g. methyglyoxyl) induces neurotoxicity to NSC-34 neurons [24]. To examine if (+)-MML1017 can protect neurons from hyperglycemic conditions, we cultured NSC-34 neuronal cells in different concentrations of glucose (0, 25, 50, 100 mM). We found that when cell viability of NSC-34 neuronal cells was significantly reduced in 100 mM glucose (Fig. 6A). We then pretreated NSC-34 neurons with or without (+)-MML1017 (25 nM) prior to 100 mM glucose incubation. We found that the cell viability of (+)-MML1017-pretreated NSC-34 was significantly higher than vehicle-pretreated NSC-34 in high glucose conditions. These data suggested that (+)-MML1017 might protect NSC-34 motor neurons from high glucose-induced apoptosis.

3.4. (+)-MML1017 stimulates calcium influx in μ-opioid receptor-expressing cells

(+)-MML1017 is a benzomorphanic derivative that possesses morphine-like activities. Activation of MOR increases cytosolic Ca^{2+} concentration. Measurement of calcium influx is an indirect way to determine MOR function. To demonstrate the (+)-MML1017 is an agonist of MOR, we performed a concentration-dependent Calcium influx assay using a MOR-expressing cell line. The results revealed that (+)-MML1017 concentration-dependently increased calcium influx. However, the agonism of (+)-MML1017 was blocked by Bevenopran, the inhibitor of periphery MOR (Fig. 7A). This indicates that (+)-MML1017 is a MOR agonist. In contrast, adipoRon did not show any apparent agonism even at a high concentration of 1 mM (Fig. 7B). These results demonstrated that (+)-MML1017 is a dual MOR- and ADIPOR-acting agonist and may be potentially more beneficial than using a single MOR agonist to treat DN.

4. Discussion

Neuroprotective effects of APN have suggested its therapeutic potential for DN. However, there is still no adiponectin-based therapy. In this study, we identified a highly potent ADIPORs agonist (+)-MML1017

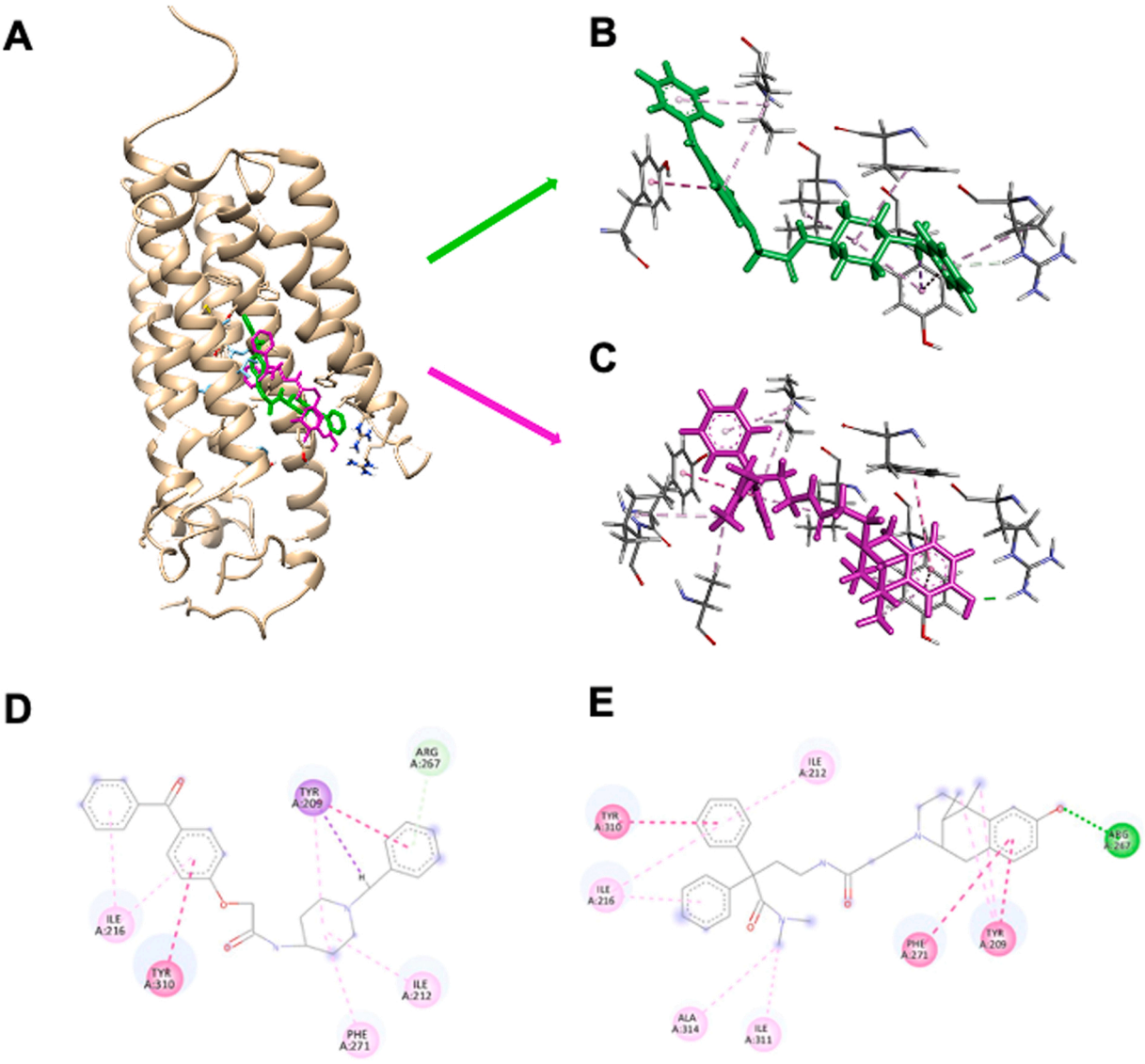

F

LIGANDS	SCORE								
ADIPORON	90.63	TYR 209	ILE 212	ILE 216	ARG 267	PHE 271	TYR 310		
(+)-MML1017	88.72	TYR 209	ILE 212	ILE 216	ARG 267	PHE 271	TYR 310	ILE 311	ALA 314

Hydrogen Bond (No-Classical)
Pi- Hydrophobic Bond
Alkyl Hydrophobic Bond
Mixed Pi/Alkyl Hydrophobic Bond

Fig. 3. Docking of AdipoRon and (+)-MML1017 into Adipo-R1 with the relevant scores. A. ADIPO-R1 is shown as solvent-accessible surface. Both AdipoRon and (+)-MML1017 bind to the same domain of ADIPO-R1. **B**. AdipoRon best pose into ADIPO-R1. AdipoRon is shown as green sticks with implicit hydrogen atoms. **C**. Best pose of (+)-MML1017 shown as magenta sticks with implicit hydrogen atoms into ADIPO-R1. **D**. AdipoRon best pose into ADIPO-R1. The specific aminoacids of ADIPO-R1 involved in the interaction. **E**. (+)-MML1017 best pose into ADIPO-R1. The specific amino acid of Adipo-R1 involved in the interaction.**F**. Best scores of AdipoRon and (+)-MML1017 best poses at ADIPO-R1. Interactions are also shown as 2D diagrams.

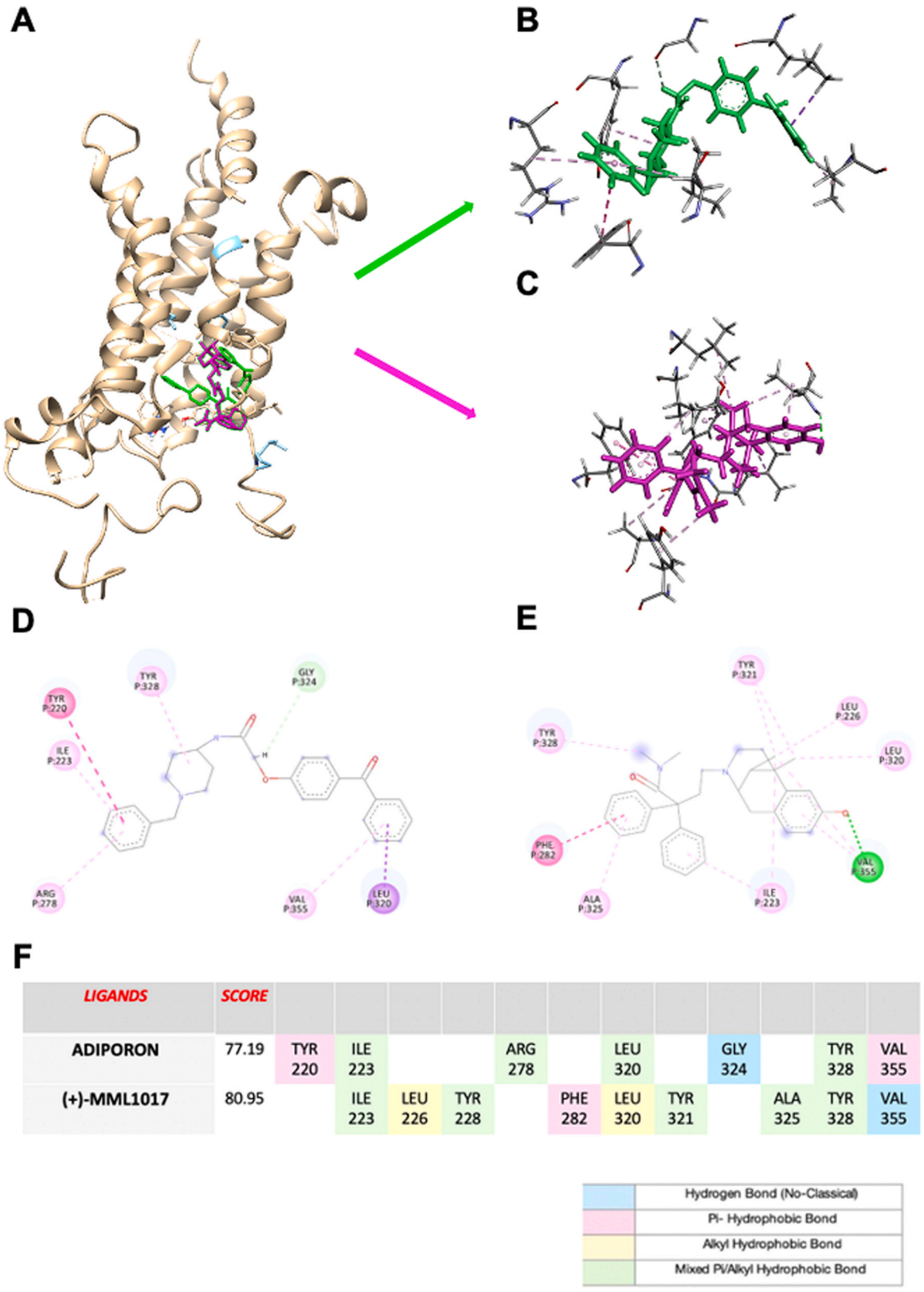

F

LIGANDS	SCORE												
ADIPORON	77.19	TYR 220	ILE 223			ARG 278		LEU 320		GLY 324		TYR 328	VAL 355
(+)-MML1017	80.95		ILE 223	LEU 226	TYR 228		PHE 282	LEU 320	TYR 321		ALA 325	TYR 328	VAL 355

	Hydrogen Bond (No-Classical)
	Pi- Hydrophobic Bond
	Alkyl Hydrophobic Bond
	Mixed Pi/Alkyl Hydrophobic Bond

Fig. 4. Docking of AdipoRon and (+)-MML1017 into ADIPO-R2. A. ADIPO-R2 is shown as solvent-accessible surface. Both AdipoRon and (+)-MML1017 bind to the same domain of ADIPO-R2. **B**. AdipoRon best pose into ADIPO-R2. AdipoRon is shown as green sticks with implicit hydrogen atoms. **C**. (+)-MML1017 best pose docked into ADIPO-R2. (+)-MML1017 is shown as magenta sticks with implicit hydrogen atoms. **D**. AdipoRon best pose docked into ADIPO-R2. The specific amino acid of ADIPO-R2 involved in the interaction are shown. **E**. (+)-MML1017 best pose into ADIPO-R2. The specific amino acid of ADIPO-R2 involved in the interaction are shown. **F**. Best scores of AdipoRon and (+)-MML1017 best poses in the interaction with ADIPO-R2. Interactions are also shown as 2D diagrams.

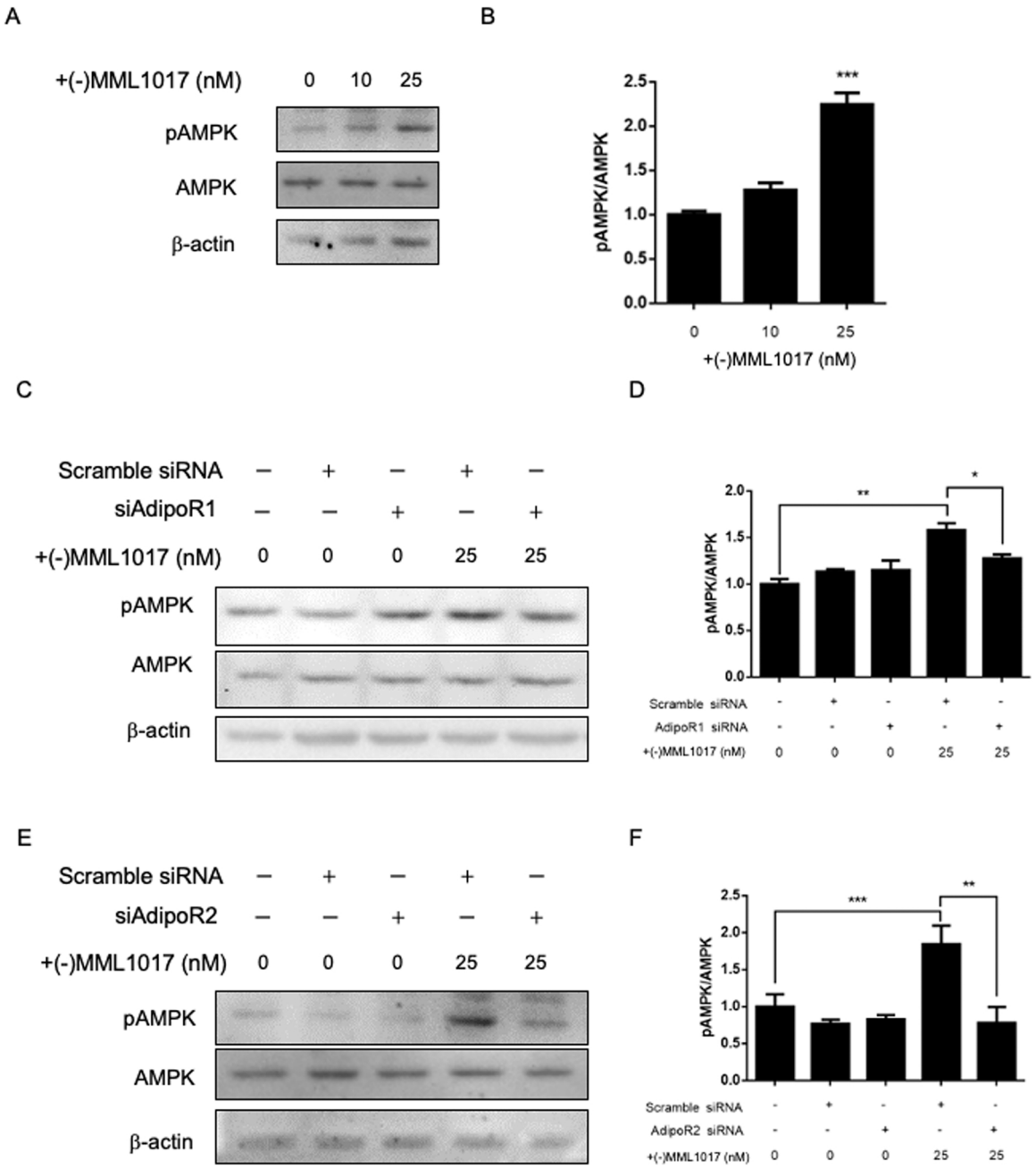

Fig. 5. Evaluation of (+)-MML1017 to induce adiponectin signaling in neuronal cell line. A. Concentration-dependent activation of AMPK, the downstream intracellular mediator of adiponectin receptors. B. Knockdown of ADIPO-R1 by siRNA blocks the activation of AMPK induced by (+)-MML1017 activities in neuronal cells. C. Knockdown of ADIPO-R2 by siRNA blocks the activation of AMPK induced by (+)-MML1017 activities in neuronal cells. All the values are expressed in s.e.m. $p < 0.05$, $p < 0.01$, $p < 0.001$ are regarded as statistically significant.

from benzomorphan derivatives that bound to the same binding domains of ADIPOR1 and ADIPOR2 as AdipoRon. (+)-MML1017 was found to increase AMPK activation and has a neuroprotective effect on hyperglycemic-induced neuronal death.

Analgesic is a common medication to relieve the symptom of neuropathic pain. Morphine binds onto opioid receptors to mediate an antinociceptive effect [7]. Benzomorphan derived from structure-activity relationships on morphine skeleton can be the pharmacological tool to explore opioid pharmacological activities. Benzomorphanic derivatives are a better option over morphine because they act as a versatile scaffold, providing modifications of functional groups that would lead to a variation of drugs such as analgesic, antiviral, anti-inflammatory, and antitumoral ligands [47]. Therefore, benzomorphanic derivatives could be multi-target ligands. As the structure of the benzomorphanic ligand library has a similar structure as adipoRon, we, therefore, hypothesize that the benzomorphanic ligands can bind to the ADIPORs. In our report, we have screened from the benzomorphan library and selected (+)-MML1017 a potent ADIPORs ligand. We have further shown that the (+)-MML1017 can activate the m-opioid receptor to increase calcium influx. Therefore, the (+)-MML1017 can be a potential dual-acting ligand of ADIPORs and MOR.

Based on the GOLD docking (Supplementary Table 1) (+)-MML1017 has a higher score (80.95) than AdipoRon (77.19) in binding to ADIPO-R2. In fact, compound (+)-MML1017 interacts with all the key residues namely PHE282, and TYR321 [32]. Overall, AdipoRon interacts with

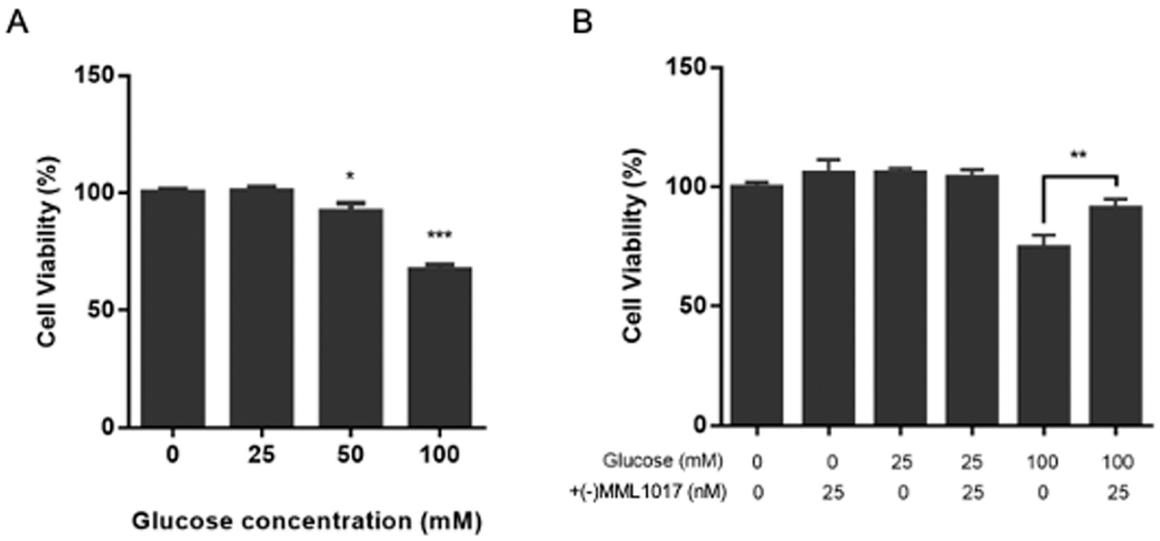

Fig. 6. (+)-MML1017 rescues hyperglycermia-induced apoptosis of NSC-34 motor neurons. A. Motor neurons were cultured with increasing concentration of glucose for 24 h prior to MTT cell viability measurement. B. Motor neurons were pretreated with 25 nM (+)-MML1017 6 h prior to hyperglycermic incubation. Cell viability was measured 24 h after incubating with glucose at different concentration. All the values are expressed in s.e.m. $p < 0.05$, $p < 0.01$, $p < 0.001$ are regarded as statistically significant.

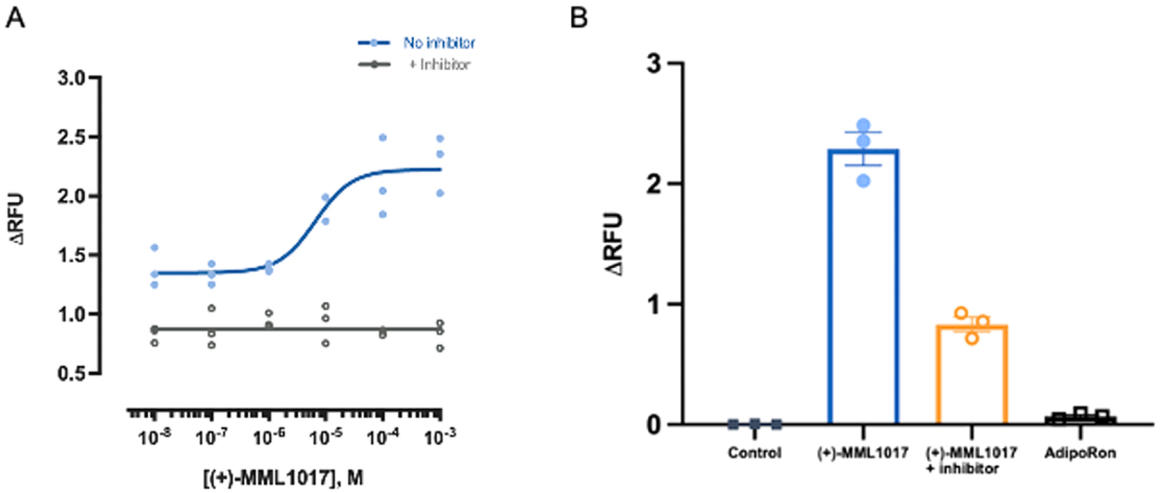

Fig. 7. (+)-MML1017 stimulates calcium influx in a concentration-dependent manner in μ-opioid expressed chem5 cells. A. Concentration-response curve for calcium influx in the fluo-8 assay evoked by increasing concentrations of (+)-MML1017 with or without μ-opioid receptor inhibitor Bevenopran. B. The calcium influx response in the presence of 1 mM (+)-MML1017, 1 mM (+)-MML1017 + 10 μM Bevenopran, and 1 mM adipoRon. RFU, relative fluorescent unit.

fewer amino acids in the active site of Adipo-R2 (TYR220, ILE233, LEU320, GLY324, TYR328) when compared to (+)-MML1017. All the interactions are hydrophobic except that with GLY324 where a hydrogen bond is formed. Thus, compound (+)-MML1017 presents a greater number of interactions with the amino acid of the active site of ADIPO-R2 than those of AdipoRon. This result can justify the high score of (+)-MML1017 compared to AdipoRon and can lead us to assume that the molecule is more active than adipoRon. Concerning the ADIPOR1 receptor, our GOLD docking results show that AdipoRon scores (90.63) and (+)-MML1017 score (88.72) are very comparable. Overall, the interactions of AdipoRon at ADIPOR1 are fewer than that of (+)-MML1017 (Fig. 3). However, the closer interactions between adipoRon and ADIPOR1 because of a reduced distance with the key amino acids might to some extent compensate for one missing interaction compared to that of the (+)-MML1017. The shorter distance then the strength of interaction can positively reflect on the GOLD docking score (4.52 Å with ARG 267 vs. 4.72 Å for (+)-MML1017; 4.71 Å with PHE271 vs. 4.85 Å for (+)-MML1017; 4.45 Å with TYR310 vs. 4.80 Å for (+)-MML1017).

Adiponectin signaling enhances insulin sensitization to improve hyperglycemia in diabetic subjects. AMPK is the major intracellular mediator of adiponectin signaling. Adiponectin activates AMPK which modulates insulin sensitization, cell survival and proliferation, fatty acid metabolism, ATP production, inflammatory responses, autophagy, and oxidative pathways [11,48]. *In vivo* studies have reported that activation of AMPK was attenuated in the peripheral nervous system of diabetic rodent models. Recent articles have demonstrated several AMPK activators can improve DN in diabetic models by promoting PGC-1α-mediated mitochondrial biogenesis, inhibiting the formation of antioxidant and oxidative stress as well as under hyperglycemic conditions [45,49,50]. In our study, we found (+)-MML1017 activates AMPK through the binding of ADIPOR1 and ADIPOR2 in a neuronal cell line that can protect against neuronal death from the hyperglycemic condition. The potential therapeutic efficacy should be further studied in vivo. However, the dual binding activity of opioid and adiponectin receptors provide additional benefit to treat diabetic neuropathy compared to

other AMPK activators.

In conclusion, we have identified a novel dual acting μ-opioid receptor and adiponectin receptor agonist, (+)-MML1017, a benzomorphan derivative, with potential neuroprotective effects. The compound activates MOR-mediated calcium influx, increases neuronal survival under hyperglycemic conditions, and activates ADIPOR-AMPK signaling. Further biochemical and pharmacological studies on preclinical models are essential to assess the potential analgesic and therapeutic benefits of (+)-MML1017 for diabetic neuropathy.

CRediT authorship contribution statement

Oscar Ka-Fai Ma: Investigation. **Simone Ronsisvalle:** Investigation, Validation. **Livia Basile:** Software, Data curation. **Ariya Weiman Xiang:** Investigation. **Cristina Tomasella:** Software, Data curation. **Federica Sipala:** Investigation, Validation. **Matteo Pappalardo:** Software, Data curation. **Koon-Ho Chan:** Writing – review & editing. **Danilo Milardi:** Writing – review & editing. **Roy Chun-Laam Ng:** Writing – original draft, Conceptualization, Methodology, Supervision. **Salvatore Guccione:** Writing – original draft, Conceptualization, Methodology, Supervision. All authors have read and revised the manuscript critically and approved the final version for publication.

Acknowledgment

CUBE LABS (CEO: Dr. Filippo Surace) and The Interuniversity Consortium “Istituto Nazionale Biostrutture e Biosistemi” (INBB – Biostructures and Biosystems National Institute) are acknowledged for the grant provided to Cristina Tomasella. University of Catania is acknowledged for the financial support open access journal “fondi di ateneo 2020–2022, Università di Catania, linea Open Access. We also thank the fundings from the University of Hong Kong (Seed funding for basic research) and Health and Medicine Research Fund (Grant no.: 08193146) granted to Dr. R. CL NG to support this project. All MD simulations were performed on resources provided by UNINETT Sigma2 - the National Infrastructure for High Performance Computing and Data Storage in Norway (http://www.sigma2.no/systems#fram).

Appendix A. Supporting information

Supplementary data associated with this article can be found in the online version at doi:10.1016/j.biopha.2022.114141.

References

[1] E.L. Feldman, K.A. Nave, T.S. Jensen, D.L.H. Bennett, New horizons in diabetic neuropathy: mechanisms, bioenergetics, and pain, Neuron 93 (2017) 1296–1313, https://doi.org/10.1016/j.neuron.2017.02.005.

[2] G.J. Francis, J.A. Martinez, W.Q. Liu, D.W. Zochodne, L.R. Hanson, W.H. Frey, C. Toth, Motor end plate innervation loss in diabetes and the role of insulin, J. Neuropathol. Exp. Neurol. 70 (2011) 323–339, https://doi.org/10.1097/NEN.0b013e318215669a.

[3] N. Niimi, H. Yako, M. Tsukamoto, S. Takaku, J. Yamauchi, E. Kawakami, H. Yanagisawa, K. Watabe, K. Utsunomiya, K. Sango, Involvement of oxidative stress and impaired lysosomal degradation in amiodarone-induced schwannopathy, Eur. J. Neurosci. 44 (2016) 1723–1733, https://doi.org/10.1111/ejn.13268.

[4] A.M. Schmeichel, J.D. Schmelzer, P.A. Low, Oxidative injury and apoptosis of dorsal root ganglion neurons in chronic experimental diabetic neuropathy, Diabetes 52 (2003) 165–171, https://doi.org/10.2337/diabetes.52.1.165.

[5] B.E. Hall, E. Macdonald, M. Cassidy, S. Yun, M.R. Sapio, P. Ray, M. Doty, P. Nara, M.D. Burton, S. Shiers, A. Ray-Chaudhury, A.J. Mannes, T.J. Price, M.J. Iadarola, A. B. Kulkarni, Transcriptomic analysis of human sensory neurons in painful diabetic neuropathy reveals inflammation and neuronal loss, Sci. Rep. 12 (2022) 1–16, https://doi.org/10.1038/s41598-022-08100-8.

[6] E. Schembri, Are opioid effective in relieving neurpathic patin, SN Compr Clin. Med (2019) 30–46, https://doi.org/10.1007/s42399-018-0009-4.

[7] M. Shaqura, B.I. Khalefa, M. Shakibaei, C. Zöllner, M. Al-Khrasani, S. Fürst, M. Schäfer, S.A. Mousa, New insights into mechanisms of opioid inhibitory effects on capsaicin-induced TRPV1 activity during painful diabetic neuropathy, Neuropharmacology 85 (2014) 142–150, https://doi.org/10.1016/j.neuropharm.2014.05.026.

[8] S. Ronsisvalle, G. Aricò, F. Panarello, A. Spadaro, L. Pasquinucci, M.S. Pappalardo, C. Parenti, N. Ronsisvalle, An LP1 analogue, selective MOR agonist with a peculiar pharmacological profile, used to scrutiny the ligand binding domain, Bioorg. Med. Chem. 24 (2016) 5280–5290, https://doi.org/10.1016/j.bmc.2016.08.057.

[9] S. Ronsisvalle, F. Panarello, A. Spadaro, S. Franchini, M. Pappalardo, S. Guccione, L. Basile, Pharmacological properties and biochemical mechanisms of μ-opioid receptor ligands might be due to different binding poses: MD studies, Future Med. Chem. 12 (2020) 2001–2018.

[10] S. Ronsisvalle, A. Spadaro, B. Tomasello, L. Basile, F. Panarello, S. Franchini, M. Renis, S. Guccione, L. Crascì, A.M. Panico, Molecular modeling and biological studies show that some μ-opioid receptor agonists might elicit analgesia acting as MMP-9 inhibitors, Future Med. Chem. 11 (2019) 1245–1258.

[11] M. Iwabu, M. Okada-Iwabu, T. Yamauchi, T. Kadowaki, Adiponectin/adiponectin receptor in disease and aging, Nat. Publ. Gr. (2015) 1–6, https://doi.org/10.1038/npjamd.2015.13.

[12] L. Vanella, G. Li Volti, S. Guccione, G. Rappazzo, E. Salvo, M. Pappalardo, S. Forte, M.L. Schwartzman, N.G. Abraham, Heme oxygenase-2/adiponectin protein-protein interaction in metabolic syndrome, Biochem. Biophys. Res. Commun. 432 (2013) 606–611, https://doi.org/10.1016/j.bbrc.2013.02.037.

[13] Y. Chen, J. Wang, L. Wang, P. Huang, Z.X. Tan, H.J. Liu, Adiponectin gene polymorphisms are associated with increased susceptibility to diabetic peripheral neuropathy, Biomarkers 20 (2015) 474–480, https://doi.org/10.3109/1354750X.2015.1101784.

[14] Z.Y. Ji, H.F. Li, Y. Lei, Y.W. Rao, Z.X. Tan, H.J. Liu, G.D. Yao, B. Hou, M.L. Sun, Association of adiponectin gene polymorphisms with an elevated risk of diabetic peripheral neuropathy in type 2 diabetes patients, J. Diabetes Complicat. 29 (2015) 887–892, https://doi.org/10.1016/j.jdiacomp.2015.06.008.

[15] K.H. Chan, K.S.L. Lam, O.Y. Cheng, J.S.C. Kwan, P.W.L. Ho, K.K.Y. Cheng, S. K. Chung, J.W.M. Ho, V.Y. Guo, A. Xu, Adiponectin is protective against oxidative stress induced cytotoxicity in amyloid-beta neurotoxicity, PLoS One 7 (2012), https://doi.org/10.1371/journal.pone.0052354.

[16] G. Qiu, R. Wan, J. Hu, M.P. Mattson, E. Spangler, S. Liu, S.Y. Yau, T.M.C. Lee, M. Gleichmann, D.K. Ingram, K.F. So, S. Zou, Adiponectin protects rat hippocampal neurons against excitotoxicity, Age 33 (2011) 155–165, https://doi.org/10.1007/s11357-010-9173-5.

[17] W. Miao, L. Jiang, F. Xu, J. Lyu, X. Jiang, M. He, Y. Liu, T. Yang, R.K. Leak, R. A. Stetler, J. Chen, X. Hu, Adiponectin ameliorates hypoperfusive cognitive deficits by boosting a neuroprotective microglial response, Prog. Neurobiol. 205 (2021), https://doi.org/10.1016/j.pneurobio.2021.102125.

[18] L. Sun, H. Li, L.W. Tai, P. Gu, C.W. Cheung, Adiponectin regulates thermal nociception in a mouse model of neuropathic pain, Br. J. Anaesth. 120 (2018) 1356–1367, https://doi.org/10.1016/j.bja.2018.01.016.

[19] J. Song, S.M. Choi, D.J. Whitcomb, B.C. Kim, Adiponectin controls the apoptosis and the expression of tight junction proteins in brain endothelial cells through AdipoR1 under beta amyloid toxicity, Cell Death Dis. 8 (2017) 1–13, https://doi.org/10.1038/cddis.2017.491.

[20] N. Kubota, W. Yano, T. Kubota, T. Yamauchi, S. Itoh, H. Kumagai, H. Kozono, I. Takamoto, S. Okamoto, T. Shiuchi, R. Suzuki, H. Satoh, A. Tsuchida, M. Moroi, K. Sugi, T. Noda, H. Ebinuma, Y. Ueta, T. Kondo, E. Araki, O. Ezaki, R. Nagai, K. Tobe, Y. Terauchi, K. Ueki, Y. Minokoshi, T. Kadowaki, Adiponectin stimulates AMP-activated protein kinase in the hypothalamus and increases food intake, Cell Metab. 6 (2007) 55–68, https://doi.org/10.1016/j.cmet.2007.06.003.

[21] I. Schamarek, C. Herder, B. Nowotny, M. Carstensen-Kirberg, K. Straßburger, P. Nowotny, A. Strom, S. Püttgen, K. Müssig, J. Szendroedi, M. Roden, D. Ziegler, Adiponectin, markers of subclinical inflammation and nerve conduction in individuals with recently diagnosed type 1 and type 2 diabetes, Eur. J. Endocrinol. 174 (2016) 433–443, https://doi.org/10.1530/EJE-15-1010.

[22] K. Muramatsu, M. Niwa, T. Tamaki, M. Ikutomo, Y. Masu, T. Hasegawa, S. Shimo, S.I. Sasaki, Effect of streptozotocin-induced diabetes on motoneurons and muscle spindles in rats, Neurosci. Res. 115 (2017) 21–28, https://doi.org/10.1016/j.neures.2016.10.004.

[23] E.L. Feldman, B.C. Callaghan, R. Pop-Busui, D.W. Zochodne, D.E. Wright, D. L. Bennett, V. Bril, J.W. Russell, V. Viswanathan, Diabetic neuropathy, Nat. Rev. Dis. Prim. 5 (2019), https://doi.org/10.1038/s41572-019-0092-1.

[24] Y.T. Tseng, H. Te Hsu, T.Y. Lee, W.H. Chang, Y.C. Lo, Naringenin, a dietary flavanone, enhances insulin-like growth factor 1 receptor-mediated antioxidant defense and attenuates methylglyoxal-induced neurite damage and apoptotic death, Nutr. Neurosci. 24 (2021) 71–81, https://doi.org/10.1080/1028415X.2019.1594554.

[25] K. Muramatsu, Diabetes mellitus-related dysfunction of the motor system, Int. J. Mol. Sci. 21 (2020) 1–26, https://doi.org/10.3390/ijms21207485.

[26] M. Okada-Iwabu, T. Yamauchi, M. Iwabu, T. Honma, K. Hamagami, K. Matsuda, M. Yamaguchi, H. Tanabe, T. Kimura-Someya, M. Shirouzu, H. Ogata, K. Tokuyama, K. Ueki, T. Nagano, A. Tanaka, S. Yokoyama, T. Kadowaki, A small-molecule AdipoR agonist for type 2 diabetes and short life in obesity, Nature 503 (2013) 493–499, https://doi.org/10.1038/nature12656.

[27] J. Bloemer, P.D. Pinky, W.D. Smith, D. Bhattacharya, A. Chauhan, M. Govindarajulu, H. Hong, M. Dhanasekaran, R. Judd, R.H. Amin, M.N. Reed, V. Suppiramaniam, Adiponectin knockout mice display cognitive and synaptic deficits, Front. Endocrinol. 10 (2019) 1–12, https://doi.org/10.3389/fendo.2019.00819.

[28] R.C.L. Ng, M. Jian, O.K.F. Ma, M. Bunting, J.S.C. Kwan, G.J. Zhou, K. Senthilkumar, A. Iyaswamy, P.K. Chan, M. Li, K.M.Y. Leung, S.S. Kumar Durairajan, K.S.L. Lam, L.W. Chu, R. Festenstein, S.K. Chung, K.H. Chan, Chronic oral administration of adipoRon reverses cognitive impairments and ameliorates

neuropathology in an Alzheimer's disease mouse model, Mol. Psychiatry (2020), https://doi.org/10.1038/s41380-020-0701-0.
[29] G. Sun, Y. You, H. Li, Y. Cheng, M. Qian, X. Zhou, H. Yuan, Q.L. Xu, L. Dai, P. Wang, K. Cheng, X. Wen, C. Chen, Discovery of AdipoRon analogues as novel AMPK activators without inhibiting mitochondrial complex I, Eur. J. Med. Chem. 200 (2020), 112466, https://doi.org/10.1016/j.ejmech.2020.112466.
[30] M.L. Verdonk, J.C. Cole, M.J. Hartshorn, C.W. Murray, R.D. Taylor, Improved protein-ligand docking using GOLD, Proteins Struct. Funct. Genet 52 (2003) 609–623, https://doi.org/10.1002/prot.10465.
[31] D.S. BIOVIA, Discov. Stud. 3 (2012) 5.
[32] M. Muratore, A.M. Komai, Theoretical study of the adiponectin receptors: binding site characterization and molecular dynamics of possible ligands for drug design, SN Appl. Sci. 2 (2020) 1–14, https://doi.org/10.1007/s42452-020-2333-z.
[33] M.R. Hestenes, E. Stiefel, Methods of conjugate gradients for solving linear systems, J. Res. Natl. Bur. Stand 49 (1952) (1934) 409, https://doi.org/10.6028/jres.049.044.
[34] H. Bouwmeester, A. Dougherty, A.V. Knyazev, Nonsymmetric preconditioning for conjugate gradient and steepest descent methods, Procedia Comput. Sci. 51 (2015) 276–285, https://doi.org/10.1016/j.procs.2015.05.241.
[35] J.R. Shewchuk, An Introduction to the Conjugate Gradient Method Without the Agonizing Pain, Pittsburgh, 1994.
[36] W. Humphrey, A. Dalke, K. Schulten, Visual molecular dynamics.Pdf, J. Mol. Graph. 14 (1996) 33–38.
[37] J.C. Phillips, R. Braun, W. Wang, J. Gumbart, E. Tajkhorshid, E. Villa, C. Chipot, R. D. Skeel, L. Kalé, K. Schulten, Scalable molecular dynamics with NAMD, J. Comput. Chem. 26 (2005) 1781–1802, https://doi.org/10.1002/jcc.20289.
[38] B.R. Brooks, C.L. Brooks, A.D. Mackerell, L. Nilsson, R.J. Petrella, B. Roux, Y. Won, G. Archontis, C. Bartels, S. Boresch, A. Caflisch, L. Caves, Q. Cui, A.R. Dinner, M. Feig, S. Fischer, J. Gao, M. Hodoscek, W. Im, K. Kuczera, T. Lazaridis, J. Ma, V. Ovchinnikov, E. Paci, R.W. Pastor, C.B. Post, J.Z. Pu, M. Schaefer, B. Tidor, R. M. Venable, H.L. Woodcock, X. Wu, W. Yang, D.M. York, M. Karplus, CHARMM: The biomolecular simulation program, J. Comput. Chem. 30 (2009) 1545–1614, https://doi.org/10.1002/jcc.21287.
[39] D.E. Tanner, J.C. Philips, K. Schulten, GPU/CPU algorithm for generalized born/solvent-accessible surface area implicit solvent calculations, Bone 8 (2012) 2521–2530, https://doi.org/10.1021/ct3003089.GPU/CPU.
[40] D.E. Tanner, K.Y. Chan, J.C. Phillips, K. Schulten, Parallel generalized born implicit solvent calculations with NAMD, J. Chem. Theory Comput. 7 (2011) 3635–3642, https://doi.org/10.1021/ct200563j.
[41] M. Okada-Iwabu, M. Iwabu, K. Ueki, T. Yamauchi, T. Kadowaki, Perspective of small-molecule AdipoR agonist for type 2 diabetes and short life in obesity, Diabetes Metab. J. 39 (2015) 363–372, https://doi.org/10.4093/dmj.2015.39.5.363.
[42] T. Yamauchi, M. Iwabu, M. Okada-Iwabu, T. Kadowaki, Adiponectin receptors: a review of their structure, function and how they work, Best. Pract. Res. Clin. Endocrinol. Metab. 28 (2014) 15–23, https://doi.org/10.1016/j.beem.2013.09.0032.
[43] R.C.L. Ng, K.H. Chan, Potential neuroprotective effects of adiponectin in Alzheimer's disease, Int. J. Mol. Sci. 18 (2017) 1–13, https://doi.org/10.3390/ijms18030592.
[44] G.R. Steinberg, D. Carling, AMP-activated protein kinase: the current landscape for drug development, Nat. Rev. Drug Discov. 18 (2019) 527–551, https://doi.org/10.1038/s41573-019-0019-2.
[45] V.G. Yerra, A. Kumar, Adenosine monophosphate-activated protein kinase abates hyperglycaemia-induced neuronal injury in experimental models of diabetic neuropathy: effects on mitochondrial biogenesis, autophagy and neuroinflammation, Mol. Neurobiol. 54 (2017) 2301–2312, https://doi.org/10.1007/s12035-016-9824-3.
[46] H. Yako, N. Niimi, A. Kato, S. Takaku, Y. Tatsumi, Y. Nishito, K. Kato, K. Sango, Role of pyruvate in maintaining cell viability and energy production under high-glucose conditions, Sci. Rep. 11 (2021) 1–17, https://doi.org/10.1038/s41598-021-98082-w.
[47] R. Turnaturi, L. Montenegro, A. Marrazzo, R. Parenti, L. Pasquinucci, C. Parenti, Benzomorphan skeleton, a versatile scaffold for different targets: a comprehensive review, Eur. J. Med. Chem. 155 (2018) 492–502, https://doi.org/10.1016/j.ejmech.2018.06.017.
[48] T. Kadowaki, T. Yamauchi, N. Kubota, K. Hara, K. Ueki, K. Tobe, Review series adiponectin and adiponectin receptors in insulin resistance, diabetes, and the metabolic syndrome, J. Clin. Invest 116 (2006) 1784–1792, https://doi.org/10.1172/JCI29126.1784.
[49] X. Xu, W. Wang, Z. Wang, J. Lv, X. Xu, J. Xu, J. Yang, X. Zhu, Y. Lu, W. Duan, X. Huang, J. Wang, J. Zhou, X. Shen, Dw14006 as a direct ampka activator ameliorates diabetic peripheral neuropathy in mice, Diabetes 69 (2020) 1974–1988, https://doi.org/10.2337/db19-1084.
[50] Q. Zhang, W. Song, B. Zhao, J. Xie, Q. Sun, X. Shi, B. Yan, G. Tian, X. Liang, Quercetin attenuates diabetic peripheral neuropathy by correcting mitochondrial abnormality via activation of AMPK/PGC-1α pathway in vivo and in vitro, Front. Neurosci. 15 (2021) 1–16, https://doi.org/10.3389/fnins.2021.636172.